~~*Appl. Sci.* **2012**, *2*, 35-45; doi:10.3390/app2010035~~

OPEN ACCESS

applied sciences

ISSN 2076-3417

www.mdpi.com/journal/applsci

Article

Steady State Analytical Equation of Motion of Linear Shaped Charges Jet Based on the Modification of Birkhoff Theory

Seokbin Lim

Energetic Systems Research Group, Department of Mechanical Engineering, New Mexico Tech, Socorro, NM 87801, USA; E-Mail: lim@nmt.edu; Tel.:+575-835-6589; Fax: +575-835-5209

Received: 5 December 2011; in revised form: 20 January 2012 / Accepted: 21 January 2012 / Published: 31 January 2012

Abstract: Birkhoff theory exhibits an analytical steady state liner collapse model of shaped charges followed by jetting process. It also provides the fundamental idea in study of shaped charges and has widened its application in many areas, including a configuration where the detonation front strikes the entire liner surface at the same time providing the $\alpha = \beta$ (liner apex angle α, and the liner collapse point angle β) condition in the literature. Upon consideration of the detonation front propagation along the lateral length of the core charge in LSCs (linear shaped charges), a further modification of the Birkhoff theory motivated by the unique geometrical condition of LSCs and the $\alpha = \beta$ condition is necessary to correctly describe the jetting behavior of LSCs which is different than that of CSCs (conical shaped charges). Based on such unique geometrical properties of LSCs, the original Birkhoff theory was modified and an analytical steady state LSCs model was built. The analytical model was then compared to the numerical simulation results created from Autodyn™ in terms of M/C ratio and apex angles in three different sized LSCs, and it exhibits favorable results in a limited range.

Keywords: linear shaped charges; explosives; detonation

1. Introduction

In the typical jet formation process of LSCs (linear shaped charges), the liner collapse process during the detonation gas expansion is an important aspect determining the performance of LSCs.

Because of the unique geometrical shape of LSCs, which are comprised of flat long liners and multiple claddings necessary in the manufacture as well as provision of confinement effects for the explosive charge, an approach to understand the performance of LSCs must be analyzed with a different perspective. For example, in a conventional application of CSCs (conical shaped charges), the top-apex initiation of CSCs followed by the gradual sweeping of detonation propagation from top to bottom of the liner provides for detonation propagation and jet projection both in the same axis, generating a focused penetration in a single-point fashion and facilitating better penetration performance. However, the linearly long-shaped LSCs, accompanied with a typical single end-point initiation, operate with different axes for the detonation propagation and the jetting projection, decreasing the penetration performance. When a detonation propagates along the length of LSCs, the interaction between the liner of LSCs and the detonation front is in a different regime than that of CSCs, creating a simultaneous projection of the entire liner without the typical gradual liner collapse occurred in CSCs.

An analytical approach of such simultaneous movement of the entire liner is described in Birkhoff theory by applying the $\alpha = \beta$ assumption, representing an identical apex and collapse angle during the liner collapse in the original equations. The resulting velocity of jetting and slug was calculated as follows [1].

$$V_j = \frac{V_p}{sin\alpha}(1 + cos\alpha) \quad (1)$$

$$V_s = \frac{V_p}{sin\alpha}(1 - cos\alpha) \quad (2)$$

where V_j, V_s, V_p, α and β are the jet, slug, liner velocity, original apex angle, and liner collapse angle respectively. Any explosive system where the $\alpha = \beta$ condition can be applied should operate according to the same concept.

Initiated from Birkhoff, there have been few publications about the motion of the LSC liner, including an analytical approximation of LSCs utilizing a vector approach [2], and the development of a numerical simulation code LESCA specifically designed for LSCs applications in combination of numerical approaches and a series of analytical approximations [3].

Analysis of the steady state liner motion of LSCs herein was motivated by the $\alpha = \beta$ condition because it describes very well the liner motion of LSCs following detonation propagation. In this paper, a steady state equation of motion of LSCs liner will be built and compared to a numerical simulation results to evaluate the applicability.

2. Steady State Equation of Motion of LSCs

In this section, the liner motion of LSCs is identified first, and a detailed steady state equation of motion will be developed based on the geometrical uniqueness of LSCs.

Upon detonation of the core charges in LSCs, the flat liner interacts with the detonation gas in a side direction creating a simultaneous movement of the entire liner at a given station along the length, maintaining the $\alpha = \beta$ condition. This is different than that of progressive liner collapse starting from top to bottom of the liner occurred in CSCs (Figure 1, Top).

This occurs at the detonation front plane at ΔOGF. However, due to the apex angle and the liner distance, the liner gradually closes the gap between liners generating a diagonal collapse line $\overline{OB}$ along

the liner while the liner collapse angle is maintained in a constant value. Assume that the diagonal collapse line $\overline{OB}$ is perpendicular to the jetting plane, and the jetting plane is under different angle with the detonation front plane ΔOGF. Because the jetting plane and the detonation plane is in different angle, the α = β condition cannot be maintained requiring a different set of apex and collapse angles (Figure 1). The α = β condition described above is only applicable in the detonation front plane ΔOGF.

Figure 1. Schematic diagram of LSC liner movement during detonation.

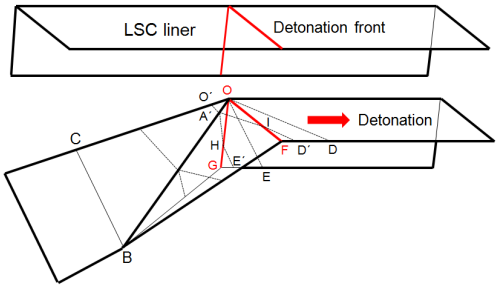

In order to develop a new set of apex and collapse angles, the specific liner collapse condition should be identified. The original apex angle α of the LSCs should be in the same plane as the detonation front plane ΔOGF. The jetting should be perpendicular to the line $\overline{OB}$ creating two jetting planes of ΔOED (before collapse starts) and A'HE′D′I (liner collapse in progress). The two planes of ΔOED and A'HE′D′I are in parallel, and these two planes bears the two important liner angles of modified apex angle before liner collapse, α′, and collapse angle β (Figure 2). Once these two angles are identified, they will be applied to the Birkhoff theory later.

Figure 2. Original apex angle α, modified apex angle before collapse α′, and collapse angles β (from left to right).

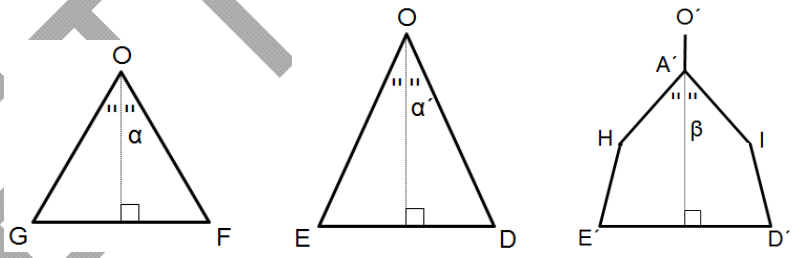

In the detonation front plane of ΔOGF where the liner collapse starts, the liner collapse completion time should be the same as time to take the liner reaches the center (1/2 $\overline{GF}$). Because we assume that the liner projects perpendicular to the liner surface with velocity V_p, the following approximated relation about t_m can be made from the Figure 3.

Figure 3. Detonation front plane and the liner projection path.

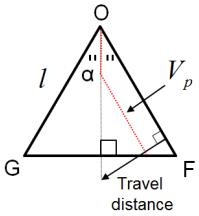

$$t_m = \frac{l\,sin\alpha}{V_p} \tag{3}$$

where, l is the liner length, and t_m is the liner collapse completion time.

The detonation front travel distance while the liner collapse completes can be calculated from the liner collapse completion time because the detonation front moves along the lateral length of the liner with the detonation velocity, D. The detonation front travel distance is $\overline{BD'}$ and Dt_m (Figure 4).

Figure 4. Jetting plane and liner.

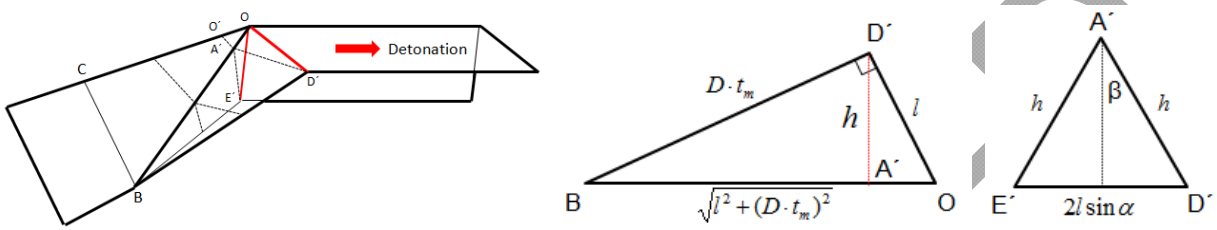

In order to find the collapse point angle, h should be identified first. From the geometrical descriptions in Figure 4, the following relations can be made.

$$\overline{OB} \times h = \overline{OD'} \times \overline{BD'} \tag{4}$$

$$h = \frac{lDt_m}{\sqrt{l^2 + (Dt_m)^2}} = \overline{A'D'} \tag{5}$$

From the jetting plane ΔA′E′D′in Figure 4, the collapse point angle β can be calculated from the following,

$$sin\beta = \frac{lsin\alpha}{h} = sin\alpha\sqrt{\left(\frac{l}{Dt_m}\right)^2 + 1} \tag{6}$$

The next step is to find the modified apex angle α′ which is different than that of the original apex angle α.

From the ΔOED in Figure 2, the length $\overline{OD}$ or $\overline{OE}$ should be identified to find α′, and the length $\overline{ED}$ is $2lsin\alpha$. Because $\overline{OB}$ is perpendicular to the jetting plane ΔOED before collapse, the following geometrical similarity relations can be made (Figure 5).

Figure 5. Geometrical similarity of ΔOCB and ΔOFD (refer to Figure 1).

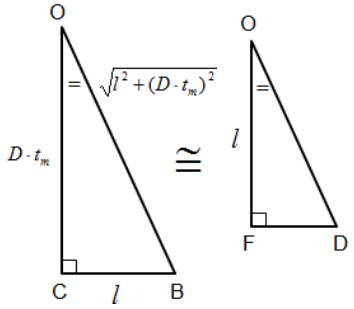

$$l : \overline{OD} = Dt_m : \sqrt{l^2 + (Dt_m)^2} \tag{7}$$

$$\overline{OD} = l\sqrt{\left(\frac{l}{Dt_m}\right)^2 + 1} \tag{8}$$

$$\sin\alpha' = \frac{\sin\alpha}{\sqrt{\left(\frac{l}{Dt_m}\right)^2 + 1}} \tag{9}$$

As a result, the collapse point angle β and the modified apex angle α′ are,

$$\beta = \sin^{-1}\left\{sin\alpha\sqrt{\left(\frac{l}{Dt_m}\right)^2 + 1}\right\} \tag{10}$$

$$\text{and } \alpha' = sin^{-1}\left\{sin\alpha/\sqrt{\left(\frac{l}{Dt_m}\right)^2 + 1}\right\} \tag{11}$$

Now, the collapse point angle β and the modified apex angle α′ are determined from the three dimensional geometrical configuration of LSCs. The next step is to apply the results in the Birkhoff theory to achieve the jet and slug velocities. Because the liner collapse behavior in the jetting plane A'HE′D′I in Figures 1 and 2 is identical to the original Birkhoff theory derivation, the following equations can be used (Figure 6).

Figure 6. Geometrical description of Birkhoff theory.

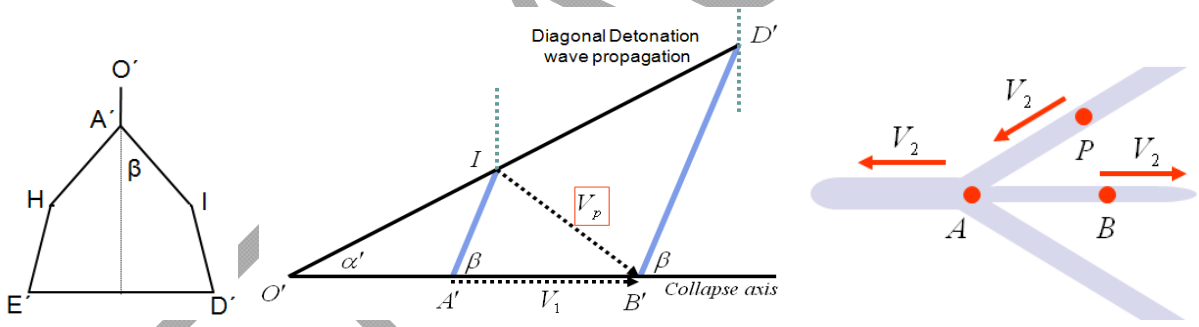

$$V_j = V_1 + V_2 = V_p\left\{\frac{sin\left(90 - \frac{\beta-\alpha\prime}{2}\right)}{sin\beta} + \frac{cos\left(\frac{\beta-\alpha\prime}{2}\right)}{tan\beta} + sin\left(\frac{\beta-\alpha'}{2}\right)\right\} \tag{12}$$

$$V_s = V_1 - V_2 = V_p\left\{\frac{sin\left(90 - \frac{\beta-\alpha\prime}{2}\right)}{sin\beta} - \frac{cos\left(\frac{\beta-\alpha\prime}{2}\right)}{tan\beta} - sin\left(\frac{\beta-\alpha'}{2}\right)\right\} \tag{13}$$

Detailed derivation of the equations is omitted to simplify the report. The only difference in between the original Birkhoff and the modified Birkhoff theory is the direction of the detonation front movement. The original Birkhoff theory assumed the sweeping detonation effect from top to the bottom of the liner. The modified Birkhoff theory, however, assumes a diagonal direction of the detonation front movement along the LSCs liner because of the different jetting and detonation front plane. This effect will be further discussed in later section.

3. Numerical Simulation and Comparison of the Results

Based on the Equations (10–13), the jet and slug velocity of typical LSCs were generated and compared to numerical simulation results created from a commercial hydrocode Autodyn™. Because there is no direct relation between the detonation and LSCs liner velocity in the equations above, the following Gurney analysis of an asymmetric open-face sandwich configuration was added in the calculation [4].

$$V_p = \sqrt{2E}\left\{\frac{\left(1+2\frac{M}{C}\right)^3+1}{6\left(1+\frac{M}{C}\right)}+\frac{M}{C}\right\}^{-0.5} \quad (14)$$

where V_p is the liner velocity, $\sqrt{2E}$ is Gurney velocity, M and C are the unit mass of liner and explosives in $\rho_0 y_0$ (density and thickness).

For the numerical simulation, the copper liner thickness was varied from 0.5, 1 and 1.5 mm, and the thickness of C4 explosives were varied to maintain the M/C values in the range of 1 to 5 with an asymmetric square shaped liner and explosives representing a reasonable size of LSCs. The material properties of the liner and explosives were determined to be identical in both theoretical and numerical calculations as shown in Table 1.

Table 1. Material properties used for the numerical simulation.

Material: Copper (liner) [5]		***Material: C4 (explosives)*** [6]	
Equation of State	***Shock***	***Equation of State***	***JWL***
Reference density	*8.96000 × 10^{-3} (kg/cm3)*	*Reference density*	*1.60100 × 10^{-3} (kg/cm3)*
Parameter C1	*3.89200 (m/ms)*	*Parameter A*	*6.09770 × 10^{-1} (TPa)*
Parameter S1	*1.48900 (none)*	*Parameter B*	*6.09770 × 10^{-1} (TPa)*
Parameter C2	*3.89200 (m/ms)*	*Parameter R1*	*4.50000 (none)*
Parameter S2	*1.48900 (none)*	*Parameter R2*	*1.40000 (none)*
Reference Temperature	*2.93000 × 10^{2} (K)*	*Parameter W*	*2.50000 × 10^{-1} (none)*
Strength	***Johnson Cook***	*C-J Detonation velocity*	*8.19300 (m/ms)*
Shear Modulus	*4.60000 × 10^{-2} (TPa)*	*C-J Energy / unit volume*	*9.00000 × 10^{-3} (kJ/mm3)*
Yield Stress	*9.00000 × 10^{-5} (TPa)*	*C-J Pressure*	*2.80000 × 10^{-2} (TPa)*
Hardening Constant	*2.92000 × 10^{-4} (TPa)*	*Burn on compression fraction*	*0.00000 (none)*
Hardening Exponent	*3.10000 × 10^{-1} (none)*	*Pre-burn bulk modulus*	*0.00000 (TPa)*
Strain Rate Constant	*2.50000 × 10^{-2} (none)*	*Adiabatic constant*	*0.00000 (none)*
Thermal Softening Exponent	*1.09000 (none)*	*Auto-convert to Ideal Gas*	*Yes*
Melting Temperature	*1.35600 × 10^{3} (K)*	*Additional Options (Beta)*	*None*
Ref. Strain Rate (/s)	*1.00000 (none)*	***Strength***	***None***
Strain Rate Correction	*1st Order*	***Failure***	***None***
Failure	***Principal Strain***	***Erosion***	***None***
Principal Tensile Failure Strain	*2.50000× 10^{-1} (none)*		
Max. Princ. Strain Difference/2	*1.01000 × 10^{20} (none)*		
Erosion	***None***		

To compare the results between the analytical calculations of the steady-state modified Birkhoff theory and the numerical simulation results, the jet velocity in the numerical simulation was measured in three different liner collapse completion rates to achieve a general tendency of the jet velocity. The jet velocity in the numerical simulation was measure at 25%, 50% and 75% of liner collapse completion stages and tabulated in Table 2, and the average values are included in Figure 7. The entire LSCs liner was designed with $\alpha = 40°$ and $l = 25$ mm.

Table 2. Modified Birkhoff and numerical simulation comparison.

Thickness (mm)		M/C	Modified Birkhoff		Jet Tip vel. in Simulation				Slug vel.
Liner	Explosives		Jet vel.	Slug vel.	25%	50%	75%	Avg.	(Simulation)
0.5	1	2.78	1.92	0.25	1.52	1.48	1.43	1.48	0.35
0.5	2	1.39	3.23	0.43	3.13	3.01	N/A *	3.01 **	0.37
0.5	3	0.93	4.17	0.55	4.5	4.3	4.2	4.33	0.5
1	1	5.56	1.06	0.14	0.6	No jet development			N/A *
1	3	1.85	2.64	0.35	3.1	2.85	N/A *	2.85 **	0.27
1	4	1.39	3.23	0.43	4.1	3.8	3.7	3.87	0.35
1	5	1.11	3.74	0.5	4.9	4.6	4.4	4.63	0.46
1	6	0.93	4.17	0.55	5.7	5.3	5.1	5.37	0.45
1.5	2	4.17	1.37	0.18	1.5	1.21	0.9	1.20	0.29
1.5	3	2.78	1.92	0.25	2.55	2.3	N/A *	2.30 **	0.17
1.5	5	1.67	2.85	0.38	4.16	3.71	N/A *	3.71 **	0.26
1.5	7	1.19	3.58	0.47	5.2	4.84	4.7	4.91	0.35
1.5	9	0.93	4.17	0.55	5.87	5.76	5.6	5.74	0.4

all velocities are in km/s. * simulation stopped due to too much deformation. ** 50% liner collapse completion value was used.

Figure 7. Modified Birkhoff and numerical simulation comparison.

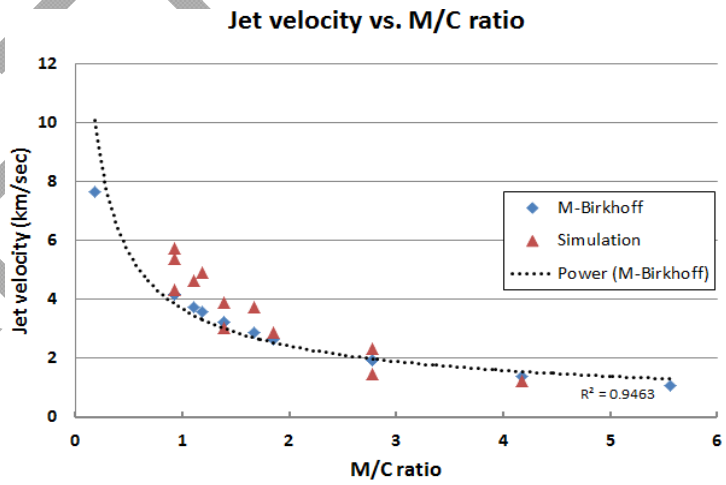

Because the modified Birkhoff theory is a steady state condition generating a single value in a single set of LSC configuration, a detailed match to the numerical simulation results having a velocity gradient is not expected. Especially, when the jet velocity during the liner collapse exhibits a nonlinear behavior, the comparison may increase significant errors. However, the average value of the jet velocity gradient during the liner collapse in 25%, 50% and 75% is almost identical to the 50% value, it is believed that the comparison is reasonable.

The comparison between the analytical calculation and the numerical simulation results shows a clear trend. The two values follow a similar curve in the entire range of M/C values, however, the values are close in higher M/C, and somewhat different in lower M/C value. One of the reasons of the differences in lower M/C range can be the rarefaction issues. In a higher M/C configuration with less explosives charge, the liner should be affected less by rarefaction effects from the explosives charges surface during the detonation, generating quite similar V_p values in between the two results.

In the lower M/C range, however, the liner should experience a significant effect from the rarefaction from the charge surface due to the comparatively large surface area, decreasing the effective charges weight [7]. Because the analytical model doesn't consider the rarefaction effects or effective charge weight in the calculation, we see differences in jet velocity between the model and the hydrocode predictions in the low-M/C range. In this case, the velocity of the modified Birkhoff theory would be larger than the simulation results, but it shouldn't be considered here without experimental data. Another issue for the difference is the under-estimation of the Gurney calculation in small M/Cs. In general the Gurney approach exhibits a gradually underestimated plate velocity below M/C = 1 and when it reaches below M/C = 0.3, it should be recognized that the Gurney results will be a lower bound for the actual velocity [8]. Because the jet velocity is greatly affected by the liner velocity, a slight change in the liner velocity may generate large differences in jetting. In addition, the sweeping detonation in the flat liner should be under the consideration of the Taylor projection angle. The modified Birkhoff theory, however, does not clearly address the issue in the derivation generating a slight change in the jet projection direction [9].

The slug velocity of the modified Birkhoff theory and the simulation results are compared as well in Figure 8.

Figure 8. Modified Birkhoff and numerical simulation comparison.

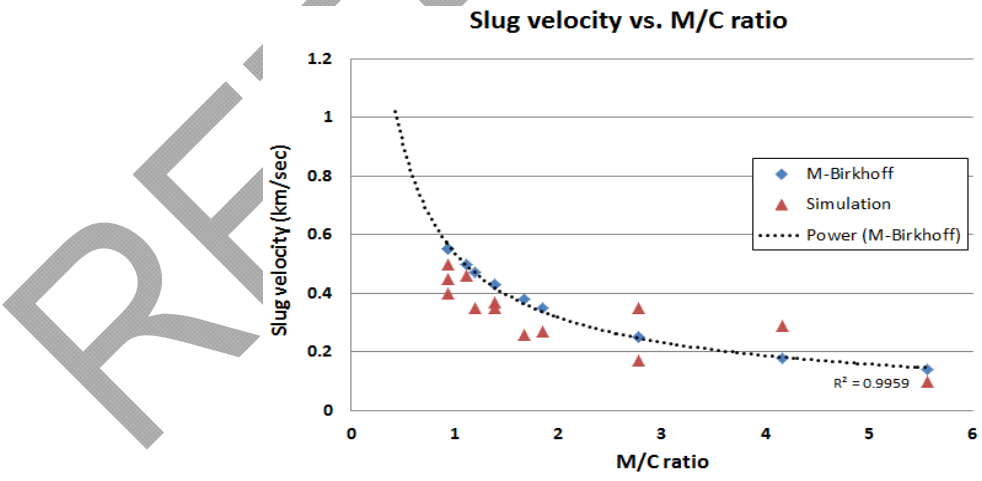

The slug velocity of the modified Birkhoff theory shows somewhat higher values in the entire range of the M/Cs than that of the simulation results. However the differences ranging from 0.04 to 0.15 km/s and ±0.08 km/s as an average difference are believed to be reasonable.

The original apex angle of LSCs is another important factor that controls the jet and slug velocities. According to the Birkhoff theory, a large apex angle creates slower jet velocity but slightly faster slug

velocity, and the same tendency can be applied to the modified Birkhoff theory as well. Results comparing dependencies of the jet and slug velocities on the original apex angles follow (Table 3).

Table 3. Modified Birkhoff and numerical simulation comparison.

Original Liner	Thickness (mm)		M/C	Modified Birkhoff		Jet Tip vel. in Simulation				Jet Tip vel.
Apex Angle, 2α (°)	Liner	Explosives		Jet vel.	Slug vel.	25%	50%	75%	Avg.	Difference
60	1	4	1.39	4.32	0.31	5.64	5.25	5.01	5.30	0.98
80	1	4	1.39	3.23	0.43	4.1	3.8	3.7	3.87	0.64
100	1	4	1.39	2.54	0.55	2.87	2.69	N/A *	2.69 **	0.15
120	1	4	1.39	2.06	0.69	2.11	2.13	N/A *	2.13 **	0.07

all velocities are in km/s. * simulation stopped due to too much deformation.** 50% liner collapse completion value was used.

The jet velocity difference between the modified Birkhoff and numerical simulation results are quite similar in the range of higher original apex angles. The differences range from 0.07 up to 0.98 km/s with the lower original apex angle exhibiting the most difference in jet velocity, and high accuracy for higher original apex angles. The reason for this difference in the range of lower original apex angle is not clearly known at this point, but it probably represents the fundamental problem of steady-state assumption that we made in the derivation. The nonlinearity of the numerical simulation produces faster jetting at smaller apex angles which cannot be described by the steady-state equation. This falls into the same regime with the comparison in Figure 7.

In summary, the comparison between the two approaches including the analytical calculation of the modified Birkhoff theory and numerical simulation results in terms of jet and slug velocity showed somewhat favorable results in a limited range depending on the original apex angle, M/C ratio and other configuration properties.

4. Discussion

Birkhoff discussed the $\alpha = \beta$ condition and subsequent changes of the original equation in the literature, and it opens another possibility of the application of such theory into LSCs. The comparison between the $\alpha = \beta$ condition in the literature and the modified Birkhoff theory described herein exhibits a definite difference. The jet velocity is almost identical in the range of over 25° of original apex angle representing the jetting plane is quite similar angle with the detonation front plane in the modified Birkhoff. However this tendency is interrupted below 25° of the original apex angle in the $\alpha = \beta$ condition (Figure 9).

The $\alpha = \beta$ condition creates a significant increase of the jet velocity near 0° original apex angle. This occurrence does not follow the theoretical results from the original Birkhoff theory, limiting its application, and the jet velocity in the range of large original apex angle decreases in general. In terms of the geometrical perspective, a LSC with a large original apex angle (close to 90°) cannot be a type of shaped charge anymore because the liner angle then creates no definite jetting. It then to EFP (Explosively Formed Projectiles) formation, with no clear jetting behavior, and the projectile (or whatever comes out of the liner surface) velocity should then be identical to the pure liner velocity calculated from Gurney analysis. Figure 10 exhibits a general jet velocity tendency of the modified

Birkhoff theory depending on the original apex angle, and it follows the liner projection tendency described above.

Figure 9. Comparison between α = β condition and the modified Birkhoff theory.

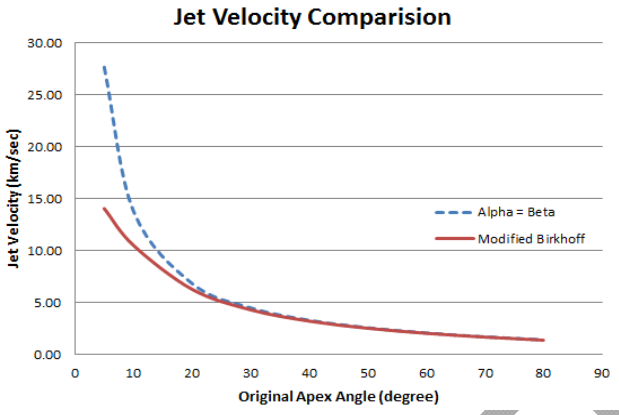

Figure 10. Jet and slug velocity depending on the original apex angle.

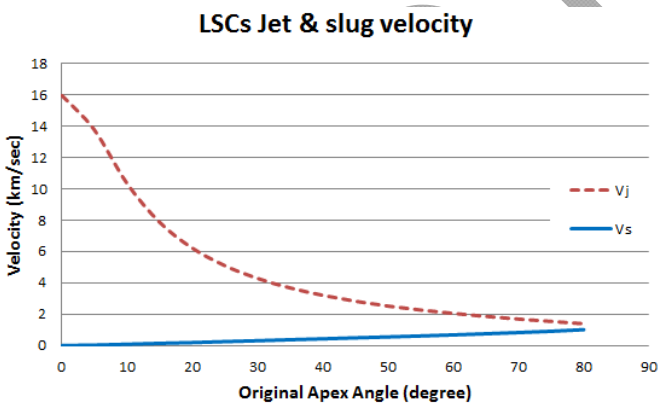

This point can be another favorable aspect of the modified Birkhoff theory because it covers both shaped charges and EFPs regime, providing all possible scenarios from the liner configuration in terms of the projectile velocity. When the original apex angles reaches to 90° the jetting process cannot occur, but the center of the flat liner bulged out due to the incoming rarefaction from the edge of the explosives surface creating a large chunk of EFP slug. In this case, the use of jetting criteria in understanding of the penetration performance wouldn't be reasonable, but a different penetration concept with an aerodynamically stable huge EFP slug capable of long distance travel should be applied. This approach is quite similar with the jet *vs.* no-jet criteria in the explosives welding application [10] in a rather different perspective.

5. Conclusions

Birkhoff theory opens an analytical approach in understanding of the shaped charge jetting process, and has been widely used for the study of shaped charges. This theory was designed for CSCs primarily. This work has developed an analytical approach for LSCs utilizing the same concept of Birkhoff theory based on the geometrical uniqueness of LSCs and the detonation front interaction with the flat liner.

In general, it is able to identify a general liner collapse behavior based on the analytical calculation of the steady-state modified Birkhoff theory. The comparison between the analytical calculation and the numerical simulation facilitates to identify the general tendency of the analytical calculation with some differences in a limited range. Due to the nature of the steady-state and non-steady-state conditions, the comparisons of the two different results probably exhibit some differences. However, the differences are limited in the given data ranges, and experimental data are necessary for more definite and further evaluation of the analytical steady-state approach.

References

1. Birkhoff, G.; Macdougall, D.P.; Pugh, E.M.; Taylor, G. Explosives with lined cavities. *J. Appl. Phys.* **1948**, *19*, 563-582.
2. Garcia, M.A. *The End-Initiated, Linear Shaped Charge: An Analytical Model*; Technical Memorandum TM-67-64; Naval Missile Center: Point Mugu, CA, USA, December 1967.
3. Robinson, A.C. *LESCA—A Code for Linear Shaped Charge Analysis*; Technical Report No. UC-742; OSTI: Albuquerque, NM, USA, 1991.
4. Gurney, R.W. *The Initial Velocities of Fragments from Bombs, Shells, and Grenades*; Army Ballistic Research Laboratory Report BRL 405; 1943.
5. Matuska, D.A. *HULL Users Manual*; AFATL-TR-84-59; June 1984.
6. Dobratz, B.M.; Crawford, P.C. *LLNL Explosives Handbook;* Report UCRL-52997 Rev.2; January 1985.
7. Baum, F.A.; Stanyukovich, K.; Shekhter, B.I. *Physics of an Explosion*; Moscow, Russia, 1959; pp. 505-507. (English translation from Federal Clearinghouse AD 400151).
8. Kennedy, J.E. *Explosive Effects and Applications*; Zukas, J., Walters, W., Eds.; Springer: Berlin, Germany, 1997; chapter 7.
9. Kennedy, J.E. Conversation, July 2011.
10. Crossland, B. *Explosive Welding of Metals and Its Application*; Oxford University Press: New York, NY, USA, 1982.